

# 1 Introduction

## 1.1 preamble

Plates are widely used in many engineering structures such as aircraft wings, ships, buildings, and offshore structures. Most plated structures, although quite capable of carrying tensile loadings, are poor in resisting compressive forces. Usually, the buckling phenomena observed in compressed plates take place rather suddenly and may lead to catastrophic structural failure. Therefore it is important to know the buckling capacities of the plates in order to avoid premature failure. The first significant treatment of plate buckling occurred in the 1800s. Based on Kirchhoff assumptions, the stability equation of rectangular plates was derived by Navier(1822). Since then, investigations on the buckling of plates with all sorts of shapes, boundary and loading conditions have been reported in standard texts (e.g. Timoshenko and Gere 1961). Research on the buckling of plates may be categorized under buckling and postbuckling. In the buckling research, it is assumed that the critical load remains below the elastic limit of the plate material. However, in practical problems the plate may be stressed beyond the elastic limit before buckling occurs. Therefore, post buckling is introduced for practical uses.

Studies on buckling analysis of plates under non-linear compressive loads have been very few. Plate problems are often idealizations of portions of a much larger overall stiffened or built-up structure-an aircraft wing or a ship or a multistoried building, for instance, and hence the loads that cause buckling are those exerted by the adjoining free –body on the plate; thus, uniform loading is an exception rather than the rule because the elastic forces between the free bodies depend on their relative stiffness. It is necessary to analyse plates subjected to various types of simple, assumed edge load distributions so as to understand their qualitative and quantitative influence on the buckling and postbuckling behavior.

The onset of “bifurcation buckling” is predicted by means of an eigen value analysis. At the buckling load, or bifurcation point on the load-deflection path, the deformations begin to grow in a new pattern, which is quite different from the pre buckling pattern. Failure, or unbounded growth of this new direction mode, occurs if the post bifurcation load-deflection curve has a negative slope and the applied load is independent of the deformation amplitude.

The postbuckled deflection curves of an axially compressed flat plate, with and without initial geometric imperfections are shown in Figs. 1.1. The curves in the figures indicate that the postbuckled equilibrium paths for flat plate are shown. It can be seen that Fig.1.1 the presence of

initial geometric imperfection  $w_0$  destroy the trivial equilibrium path, and we have now a family of stable equilibrium curves corresponding to different values of  $w_0$  that round off the bifurcation of the perfect system.

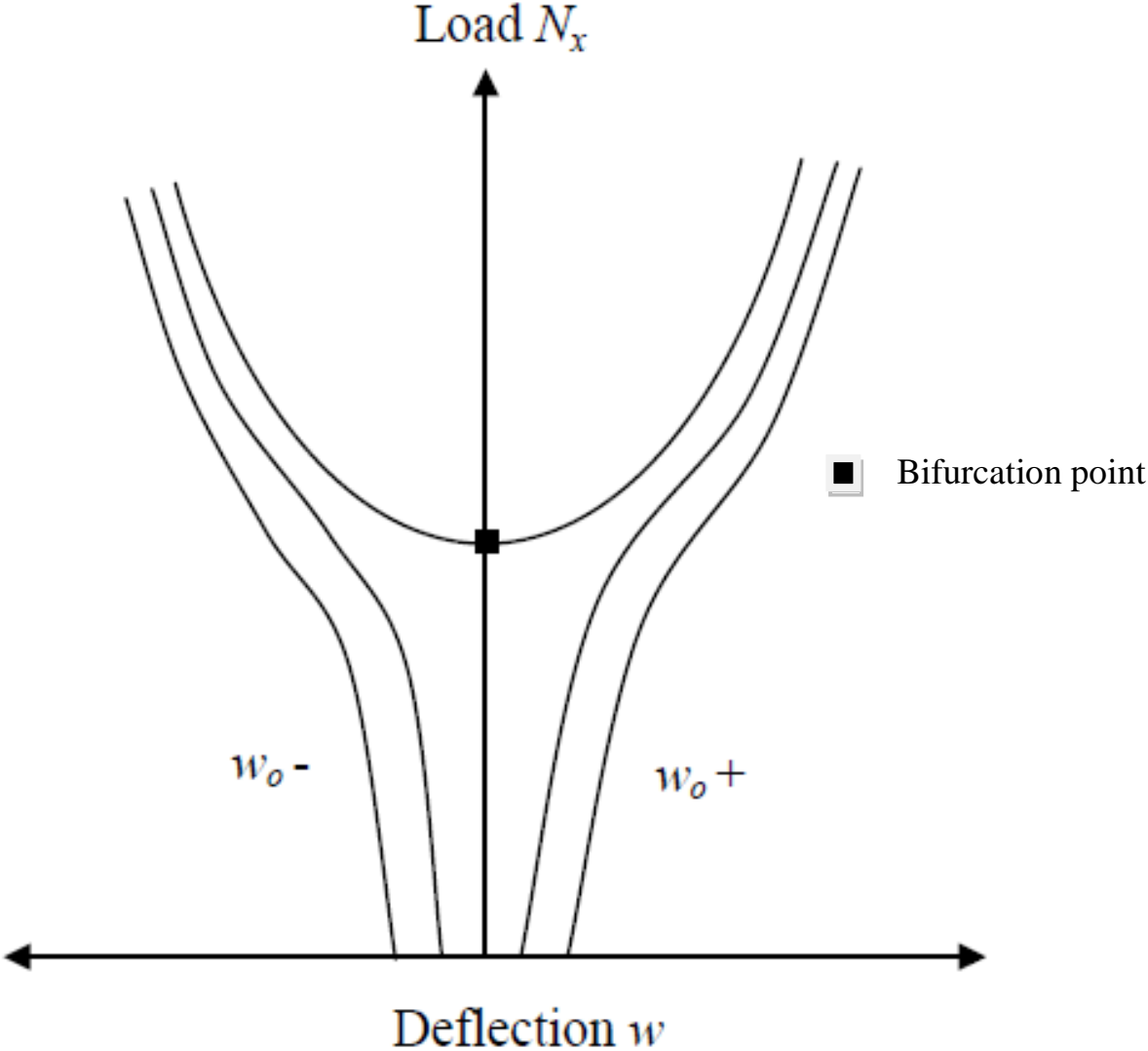


Fig .1.1 postbuckled deflection curves showing bifurcation points under uniaxial compression of perfect and Imperfect plate

## 1.2 Objective

The objective of the present study is to investigate the buckling and postbuckling of thin plates and to obtain accurate analytical results using multi-term Galerkin's method for a wide range of loading and structural parameters.

## 1.3 Scope of the studies :

### 1.3.1 Loading condition

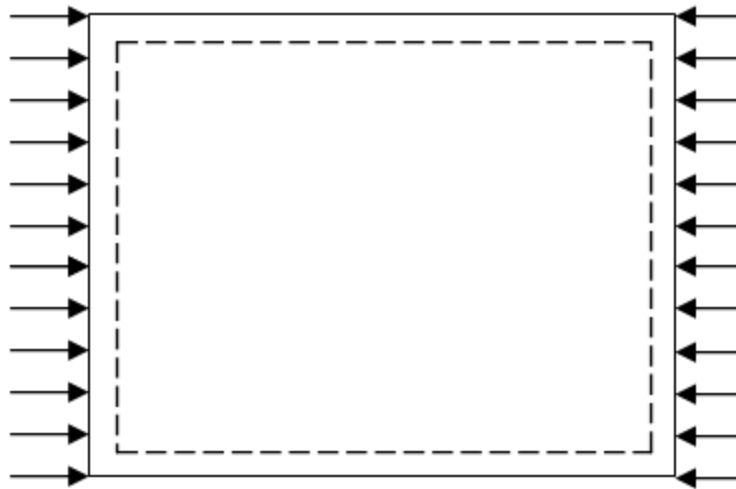


Fig. 1.3.1 Plate is subjected to uniformly distributed load

### 1.3.2 Different boundary condition

### 1.3.3 Isotropic plate

### 1.3.4 Plate with imperfection

## 1.4 Contribution

It is observed from the literature that, a large volume of research work (Timoshenko and Gere, 1963); exists in the area of buckling, postbuckling, of isotropic plates. In this work, the governing partial differential equations for plate by various variational principle. The critical buckling loads and postbuckling are evaluated for isotropic plates subjected to uniform in-plane loadings considering different boundary conditions. Postbuckling equilibrium

paths of simply supported isotropic plates subjected to uniform in-plane compressive edge loads and lateral loads are traced. It is observed from the above discussion that buckling and postbuckling of isotropic plates. The detailed review of literature in this field along with the critical discussion is presented in the next chapter based on which objective and scope of the present investigation is identified.

## **2 Literature Review**

In the following, a literature review on the buckling of rectangular plates is presented to provide the background information for the present investigation. The review focuses on homogenous, isotropic, thin plates.

### **2.1 Buckling of rectangular plates**

This part is concerned with the research done for the buckling of rectangular plates under various in-plane loads and boundary conditions for the plate edges. Navier (1822) derived the basic stability equation for rectangular plates under lateral load by including the twisting action. The inclusion of the 'twisting' term is very important because the resistance of the plate to twisting can considerably reduce deflections under lateral load. Saint-Venant (1883) modified the equation by including axial edge forces and shearing forces. The modified equation formed the basis for much of the work on plate stability of plates with various loads and boundary equation of equilibrium. More recently, Reddy (1999) applied the Rayleigh-Ritz approximation to solve the CCCC plates under shear forces.

Batdorf and Stein (1947) evaluated the buckling problem under combined shear and compression combinations for simply supported plates by adopting the deflection function in the form of infinite series. Batdorf and Houbolt (1946) gave a solution to the equation of equilibrium for infinitely long plates with restrained edges under shear and uniform transverse compression. Johnson and Buchert (1951) used the energy method to explore the buckling behavior of rectangular plates with compression edge simply supported or elastically restrained, tension edge simply supported. Researchers who are interested in this field of research may refer to Bulson (1970), in which many research papers were cited. More recently, Kang and Leissa (2001) presented exact solutions for the buckling of rectangular plates having two opposite, simply supported edges subjected to linearly varying normal stresses causing pure in-plane moments, the other two edges being free.

Farvre (1948) is probably the first researcher to work out approximate buckling solutions of rectangular plates under self weight and uniform in-plane compressive forces. However, he treated only plates with all four edges simply supported. Wang and Sussman(1967) solved the same problem using the Rayleigh-Ritz method and concluded that the average stress in the plate at buckling is less than that for a plate with uniform compression at buckling. Both Favre (1948) and Wang and Sussman (1967) did not give numerical values in their papers. Using the

conjugate load-displacement method, Brown (1991) investigated the buckling of rectangular plates under (a) a uniformly distributed load, (b) a linearly increasing distributed load and (c) a varying sinusoidal load across the plate width. The second type of load is equivalent to the plate's self weight. In his study, Brown treated a number of combinations of boundary conditions. More recently, Wang et al. (2002) considered the buckling problem of vertical plates under body forces/self weight. The vertical plate is either clamped or simply supported at its bottom edge while its top edge is free. The two sides of the plate may either be free, simply supported or clamped. Xiang et al. (2003) treated yet another new elastic buckling problem where the buckling capacities of cantilevered, vertical, rectangular plates under body forces are computed. Buckling of plates under other forms of loads Bulson cited Yamaki's buckling studies on SSSS, CSCS and CCCC plates under equal and opposite point loads as shown in Fig. 2.1a. Bulson (1970) also cited Yamaki's research on buckling problems of CSCS and SSSS plates under partially distributed loads which are acted upon the simply supported edges as shown in Fig. 2.1b. Lee et al. (2001) considered the buckling problem of square EEEE and ESES plates subjected to in-plane loads of different configurations acting on opposite sides of plates as shown in Figs 2.1c and 2.1d. The effects of Kinney's fixity factor (introduced to describe the support conditions at the edges covering the boundary conditions of simply supported and fixed edges) and the width factor on critical load factors were treated.

Sarat and Ramachandra (2010) studied the effects of boundary conditions, non-uniform in plane loading, plate aspect ratio and length/thickness ratio on the buckling behavior of rectangular composite plates.

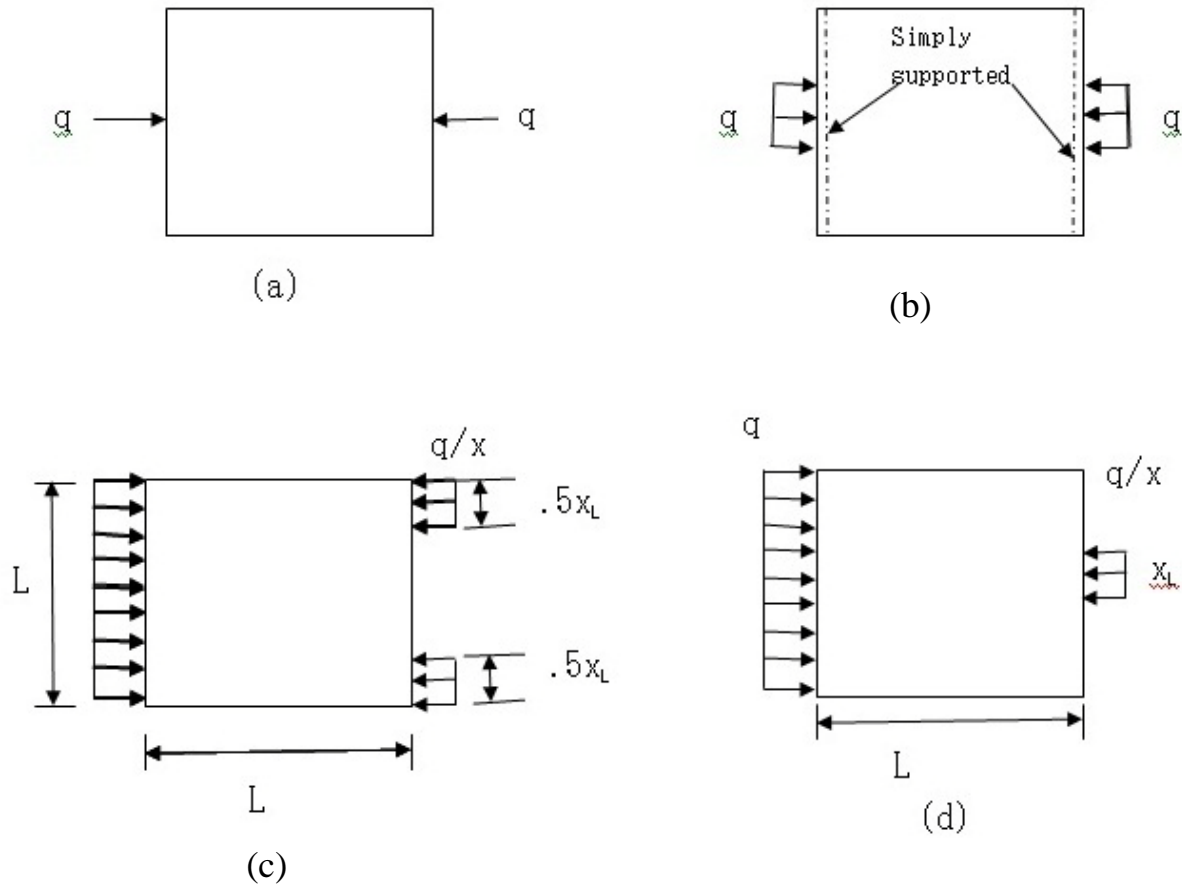


Fig. 2.1 plates under (a) points loads; (b) partially distributed load ;(c) patch loads at edge center; (d) patch loads near corners

## 2.2 Post buckling of rectangular plates:

This part is concerned with the development of the plastic stability theories. Incremental theory of plasticity (IT) and the deformation theory of plasticity (DT) are considered in detail. As an alternative method, the strip method is also briefly reviewed. The earliest development of DT is due to Engesser (1895) and Von Karman (1910). They developed a theory based on the fact that for a fiber which is compressed beyond the elastic limit, the tangent modulus (i.e. the ratio of the variation of strain to the corresponding variation of stress) assumes different values depending on whether the variation of stress constitutes an increase or a relief of the existing compressive stress.

Bleich (1924) and Timoshenko (1936) applied Engesser-Von Karman theory to the plastic buckling of plates by introducing the “reduced modulus” into the formulas for the elastic

buckling of plates. The results of their theory were obtained in the case of an arrow rectangular strip with its compressed short edge simply supported and the long edges free. Kaufmann (1936) and Ilyushin (1944) developed the basis of deformation theory of plasticity by presenting another route for application of Engesser-Von Karman theory. They went back to the considerations by which the reduced modulus was derived and applied to the case of buckled a plate. Ilyushin (1946) reduced the problem to the solution of two simultaneous nonlinear partial differential equations of the fourth order in the deflection and stress function, and in the approximate analysis to a single linear equation. Solutions were given for the special cases of a rectangular plate buckling into a cylindrical form, and of an arbitrarily shaped plate under uniform compression. Stowell(1948) assumed that the plate remained in the purely plastic state during buckling. He used Ilyushin's general relations to derive the differential equation of equilibrium of plates under combined loads. The corresponding energy expressions were also found. Bijlaard (1949) also used the assumption of "plastic deformation". He derived the stress-strain relations by writing the infinitely small excess strains as total differentials and computing the partial derivatives of the strains with respect to the stresses. The differential equation for plate buckling was derived and results of its application to several kinds of loading and boundary conditions were given. El-Ghazaly and Sherbourne (1986) employed the deformation theory for the elastic-plastic buckling analysis of plates under non-proportional external loading and non-proportional stresses. Loading, unloading, and reloading situations were considered. Comparison between experiments and analysis results showed that the deformation theory of plasticity was applicable insituations involving plastic buckling under non-proportional loading and non-uniform stress fields. The incremental theory of plasticity was first developed in the early work by Handelman and Prager (1948). They assumed that for a given state of stress there existed a one-to-one correspondence between the rates of change of stress and strain in such a manner that the resulting relation between stress and strain cannot be integrated so as to yield a relation between stress and strain along. Pearson (1950) modified Handelman and Prager's assumption of initial loading. His analytical results showed that the incremental was improved by incorporating Shanley's concept of continuous loading. Deformation theory and incremental theory of plasticity are two competing plastic theories. Consequently much work and comparison studies have been done by using both of them. Shrivastava (1979) analyzed the inelastic buckling by including the effects of transverse shear by both theories. Three cases were discussed: (1) for



infinitely long simply supported plates, (2) for square simply supported plates, and (3) for infinitely long ones simply supported on three sides and free on one unloaded edge. Ore and Durban (1989) presented a linear buckling analysis for annular elastoplastic plates under shear loads. They found that deformation theory predicts critical loads which were considerably below the predictions obtained with the flow theory. Furthermore, comparison with experimental data for different metals showed a good agreement with the deformation theory. Tugcu (1991) employed both theories for simply supported plates under biaxial loads. It was shown that the incremental theory predictions for the critical buckling were susceptible to significant reductions due to a number of factors pertinent to testing, while the deformation theory analysis was shown to be more or less insensitive to all of these factors. Durban and Zuckerman (1999) examined the elasto plastic buckling of a rectangular plate with three sets of boundary conditions (four simply supported boundaries and the symmetric combinations of clamped/simplely supported sides). It was found that for thicker plates, the deformation theory gives lower critical stresses than those obtained from the incremental theory. There is a general agreement among engineers and researchers that (a) deformation theory is physically less correct than incremental theory, but (b) deformation theory predicts buckling loads that are smaller than those obtained with incremental theory, and(c) experimental evidence points in favor of deformation theory results. Onat and Drucker (1953) through an approximate analysis showed that incremental theory predictions for the maximum support load of long plates supported on three sides will come down to the deformation theory bifurcation load if small but unavoidable imperfections were taken into account. Later, the plate buckling paradox was examined by Sewell (1963) who obtained somewhat lower flow theory buckling loads by allowing a variation in the direction of the unit normal. Sewell (1973) in a subsequent study illustrated that use of Tresca yield surface brings about significant reductions in the buckling loads obtained using incremental theory. Neale (1975) examined the sensitivity of maximum support load predictions to initial geometric imperfections, using incremental theory. A similar study was performed by Needleman and Tvergaard (1976) which also included the effect of in-plane boundary conditions for square plates under uniaxial compression. An exhaustive discussion of the buckling paradox in general is given by Hutchinson (1974). While imperfection sensitivity provided a widely accepted explanation for the buckling paradox in general, reservations concerning the mode and amplitude of the imposed imperfections for some buckling problems are not uncommon. Readers who are

interested in plastic buckling of plates may obtain further information from these published papers: Wang (2003). From the literature review above, we can see that although much work has been done, the buckling of rectangular plates subjected to end and intermediate loads remain hitherto untouched. This has prompted the author to work on this project.

An analysis of the elastic postbuckling response of biaxially compressed plates was carried out by Steen et al. (2008) with main focus on change of in-plane postbuckling stiffness under prescribed plate end shortenings rather than the load control. Basagni and Vescovini (2009) presented an analytical formulation for the study of linearized local skin buckling load and nonlinear postbuckling behavior of isotropic and composite stiffened panel under axial compression. Authors concluded that the analysis is best suited to be used in optimization routine for preliminary design. A finite element formulation of Koiter's initial postbuckling theory using a multi mode approach was investigated by Rahman and Jansen (2009). They illustrated the capability of method by analyzing the buckling of shell structures including modal interaction.

## **3Mathematical Formulation**

### **3.1 Introduction**

In this chapter, the partial differential equations governing the buckling and postbuckling of isotropic plates are derived from variational principles. The governing partial differential equations in two independent variables are derived via variational principles. Usually one could formulate the governing partial differential equations in three independent variables (as in three-dimensional elasticity) or in two variables (as in the case of two-dimensional models). In the present case, two-dimensional approach has been adopted to model of plates. The dimensional reduction is achieved by mapping all mechanical variables (such as body forces, strains and stresses) from three-dimensions to two-dimensions making use of the across the thickness assumption. The multi-term Galerkin's procedure adopted for solving partial differential equations is also discussed. The governing partial differential equations governing the buckling and postbuckling isotropic plates are derived from variational principle in this chapter adopting higher order shear deformation theory (Reddy, 2002, 2007) and including von Karman type of nonlinearity.

### **3.2 The Von Karman theory of plates**

In this section we shall derive the Von Karman theory of plates. This is a nonlinear theory that allows for comparatively large rotations of line elements originally normal to the x, y axes in the mid plane of the plate (figure 3.2.1). These rotations terms allow projections of the in- plane forces  $\overline{N}_v$  and  $\overline{N}_{vs}$  to be felt in the transverse direction, normal to the plane of plate.

This theory is derive assuming that strains and rotations are both small compared to unity, so that we can ignore changes in geometry in the definition of stress components and in the limits of integration needed for work and energy considerations. We further stipulate that the strains will be smaller than the rotations, in the sense described below.

We introduce the linear strain parameters  $e_{ij}$  and the rotation parameters  $\omega_{ij}$  defined as

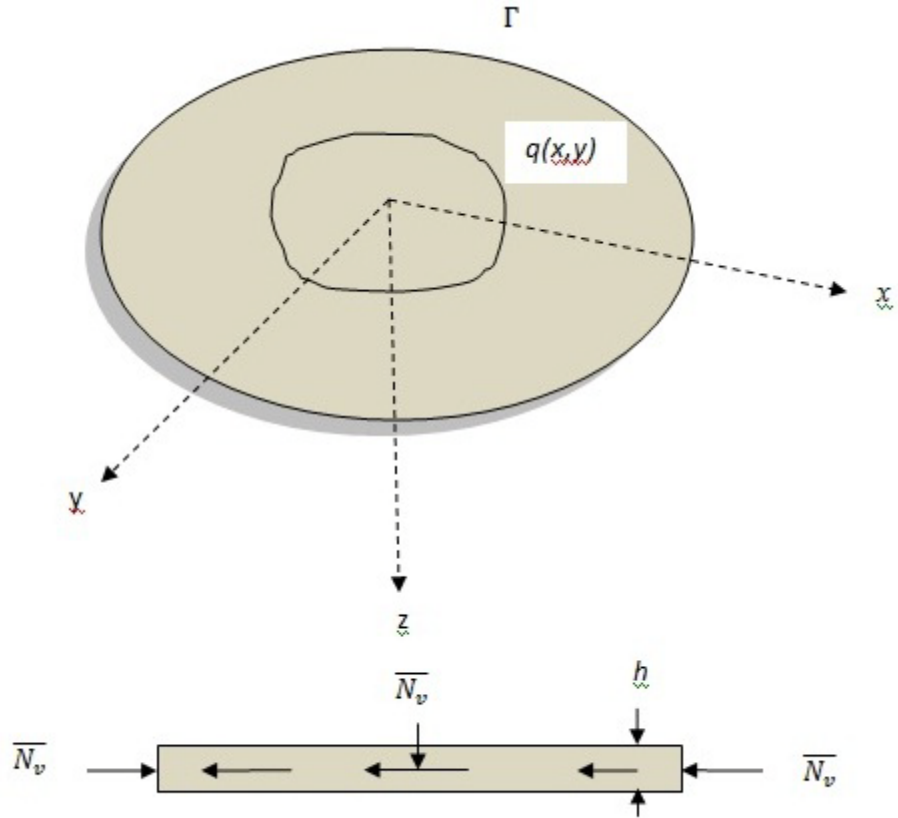


Fig.3.2.1

$$2e_{ij} = u_{i,j} + u_{j,i} \quad (3.2.1)$$

$$2\omega_{ij} = u_{i,j} - u_{j,i} \quad (3.2.2)$$

$$2\epsilon_{ij} = 2e_{ij} + (e_{ki} + \omega_{ki})(e_{kj} + \omega_{kj}) \quad (3.2.3)$$

For simplification discussed, namely  $e_{ki} \ll \omega_{ki}$  reduces to

$$\epsilon_{ij} = e_{ij} + \frac{1}{2}\omega_{ki} * \omega_{ki} \quad (3.2.4)$$

Finally Kirchhoff assumption that lines normal to undeformed middle surface remain normal to this surface in the deformed geometry and are not extended after deformation. That means

$$u_1(x_1, x_2, x_3) = u(x, y) - z \frac{\partial w(x, y)}{\partial x} \quad (3.2.5)$$

$$u_2(x_1, x_2, x_3) = v(x, y) - z \frac{\partial w(x, y)}{\partial y} \quad (3.2.6)$$

$$u_3(x_1, x_2, x_3) = w(x, y) \quad (3.2.7)$$

Where  $u$ ,  $v$  and  $w$  are the displacement components of the middle surface of the plate. We may now give strain parameters and rotation parameters as follows:

$$\begin{aligned} e_{11} &= \frac{\partial u}{\partial x} - z \frac{\partial^2 w}{\partial x^2} \\ e_{12} &= \frac{1}{2} \left( \frac{\partial u}{\partial y} + \frac{\partial v}{\partial x} - 2z \frac{\partial^2 w}{\partial x \partial y} \right) \\ e_{22} &= \frac{\partial v}{\partial y} - z \frac{\partial^2 w}{\partial y^2} \end{aligned} \quad (3.2.8a)$$

$$e_{13} = e_{23} = 0$$

$$\omega_{12} = \frac{1}{2} \left( \frac{\partial u}{\partial y} - \frac{\partial v}{\partial x} \right)$$

$$\omega_{13} = \frac{\partial w}{\partial x} \quad (3.2.8b)$$

$$\omega_{23} = \frac{\partial w}{\partial y}$$

We now observe the following. The rotation parameter  $\omega_{12}$  approximates a rotation component about the  $z$  axis, while rotation components about axes parallel to the  $x$  and  $y$  axes, respectively, in the mid plane of the plate. For a thin, hence flexible, plate we can reasonably expect that:

$$\omega_{12} \ll \omega_{23}, \omega_{13} \quad (3.2.9)$$

Neglecting  $\omega_{12}$ , we can now employ Eqs.3.2.4 and 3.2.8 to find the  $\epsilon_{ij}$ :

$$\epsilon_{11} = \frac{\partial u}{\partial x} - z \frac{\partial^2 w}{\partial x^2} + \frac{1}{2} \left( \frac{\partial w}{\partial x} \right)^2$$

$$\begin{aligned}\epsilon_{22} &= \frac{\partial v}{\partial y} - z \frac{\partial^2 w}{\partial y^2} + \frac{1}{2} \left( \frac{\partial w}{\partial y} \right)^2 \\ \epsilon_{33} &= \frac{1}{2} \left( \frac{\partial w}{\partial x} \right)^2 + \frac{1}{2} \left( \frac{\partial w}{\partial y} \right)^2\end{aligned}\quad (3.2.10)$$

$$\epsilon_{12} = \frac{1}{2} \left( \frac{\partial u}{\partial y} + \frac{\partial v}{\partial x} - 2z \frac{\partial^2 w}{\partial x \partial y} \right) + \frac{1}{2} \frac{\partial w}{\partial x} \frac{\partial w}{\partial y}$$

$$\epsilon_{13} \cong \epsilon_{23} \cong 0$$

For a constitutive law we will employ Hook's law for plane stress over the thickness of the plate. Thus we shall be concerned here only with  $\epsilon_{11}$ ,  $\epsilon_{22}$  and  $\epsilon_{12}$ . Accordingly, for the assumptions presented here, we can say that the first variation of strain energy  $U$  is

$$\begin{aligned}\delta^{(1)}U &= \iiint_V \tau_{ij} \delta \epsilon_{ij} dv \\ &= \iint_R \int_{-h/2}^{h/2} (\tau_{11} \delta \epsilon_{11} + 2\tau_{12} \delta \epsilon_{12} + \tau_{22} \delta \epsilon_{22}) dz dA\end{aligned}\quad (3.2.11)$$

Now we replace the strain terms in the above expression and commute the delta operator with derivative operators.

$$\begin{aligned}\delta^{(1)}U &= \iint_R \int_{-h/2}^{h/2} \left\{ \tau_{11} \left( \frac{\partial \delta u}{\partial x} + \frac{\partial w}{\partial x} \frac{\partial \delta w}{\partial x} - z \frac{\partial^2 \delta w}{\partial x^2} \right) + \left( \frac{\partial \delta u}{\partial y} + \frac{\partial \delta v}{\partial x} - 2z \frac{\partial^2 \delta w}{\partial x \partial y} + \right. \right. \\ &\left. \left. \frac{\partial w}{\partial x} \frac{\partial \delta w}{\partial y} + \frac{\partial w}{\partial y} \frac{\partial \delta w}{\partial x} \right) + \tau_{22} \left( \frac{\partial \delta v}{\partial y} + \frac{\partial w}{\partial y} \frac{\partial \delta w}{\partial y} - z \frac{\partial^2 \delta w}{\partial y^2} \right) \right\} dA dz\end{aligned}\quad (3.2.12)$$

Next we integrate with respect to  $z$  and introduce resultant stress and moment intensity functions  $N_x$ ,  $N_y$  and  $N_{xy}$ , and  $M_x$ ,  $M_y$ , and  $M_{xy}$  respectively:

$$\begin{aligned}M_x &= \int_{-h/2}^{h/2} \tau_{xx} z dz \\ M_y &= \int_{-h/2}^{h/2} \tau_{yy} z dz \\ M_{xy} &= \int_{-h/2}^{h/2} \tau_{xy} z dz = M_{xy}\end{aligned}\quad (3.2.13)$$

$$N_x = \int_{-h/2}^{h/2} \tau_{xx} dz$$

$$N_y = \int_{-h/2}^{h/2} \tau_{yy} dz$$

$$N_{xy} = \int_{-h/2}^{h/2} \tau_{xy} dz = N_{yx}$$

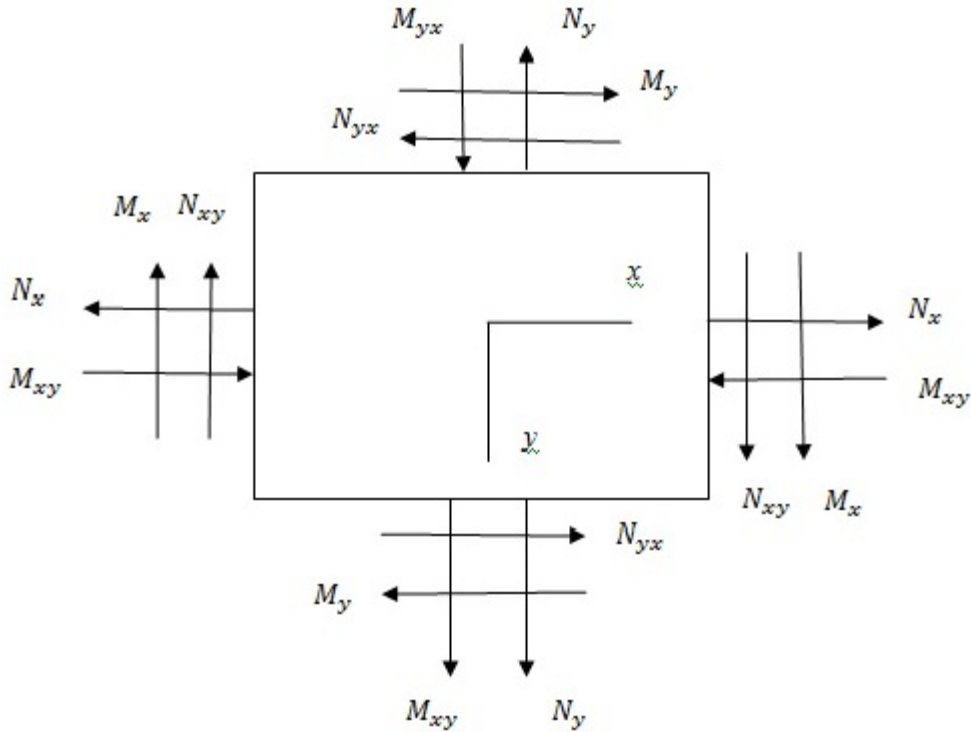


Fig.3.2.2

Where  $N_x$  ( $N_y$ ), as shown in the figure3.2.2 is a force in the x direction (y direction) measured per unit length in the y direction (x direction) and where  $N_{xy}$  ( $N_{yx}$ ) is a force in the x(y) direction per unit length in the y(x) direction. Similarly, the quantity  $M_x$  represents a moment per unit length in the y direction, with its vector in the y direction. Finally,  $M_{xy}$  is the twisting moment per unit length in the y direction with its vector in the x direction. The terms  $N_x$ ,  $N_y$ ,  $N_{xy}$  and  $N_{yx}$  may for practical purposes be compared with normal and shear stresses and we may conclude that  $N_{xy} = N_{yx}$  then we got the following result:

The Eqs(3.2.12) can be written as

$$\delta^{(1)}U = \iint_R \left[ N_x \left( \frac{\partial \delta u}{\partial x} + \frac{\partial w}{\partial x} \frac{\partial \delta w}{\partial x} \right) - M_x \frac{\partial^2 \delta w}{\partial x^2} + N_{xy} \left( \frac{\partial \delta u}{\partial y} + \frac{\partial \delta v}{\partial x} + \frac{\partial w}{\partial x} \frac{\partial \delta w}{\partial y} + \frac{\partial w}{\partial y} \frac{\partial \delta w}{\partial x} \right) - 2M_{xy} \frac{\partial^2 \delta w}{\partial x \partial y} + N_y \left( \frac{\partial \delta v}{\partial y} + \frac{\partial w}{\partial y} \frac{\partial \delta w}{\partial y} \right) - M_y \frac{\partial^2 \delta w}{\partial y^2} \right] dx dy \quad (3.2.14)$$

The first variation of the potential of the applied forces meanwhile takes the form noting that  $\overline{N}_v$  is taken as positive in compression as shown in the figure.

$$\delta^{(1)}V = -\iint_R q \delta w dx dy + \oint_r \overline{N}_v \delta u_v ds + \oint_r \overline{N}_{vs} \delta u_s ds \quad (3.2.15)$$

Where  $u_v$  and  $u_s$  are the in plane displacements of the boundary of the plate in direction normal and tangential to the boundary, respectively. We are using the under formed geometry for the applied loads above rather than the deformed geometry thereby restricting the result to reasonably small deformations. By using the above result for  $\delta^{(1)}V$  and using equation 3.2.14 for  $\delta^{(1)}U$ , may be form  $\delta^{(1)}\pi$ . The total potential energy so formed approximates the actual total potential energy for the kind of deformation restrictions embodied in kirchhoff's assumptions. And since we have used under formed geometry for stresses and external loads, we are limited to small deformations in employing this functional. Finally, because we used equation 3.2.4 for strain, we are assuming that strains are much smaller than rotations. Thus we have for the total potential energy principle:

$$\delta^{(1)}\pi = U = \iint_R \left[ N_x \left( \frac{\partial \delta u}{\partial x} + \frac{\partial w}{\partial x} \frac{\partial \delta w}{\partial x} \right) - M_x \frac{\partial^2 \delta w}{\partial x^2} + N_{xy} \left( \frac{\partial \delta u}{\partial y} + \frac{\partial \delta v}{\partial x} + \frac{\partial w}{\partial x} \frac{\partial \delta w}{\partial y} + \frac{\partial w}{\partial y} \frac{\partial \delta w}{\partial x} \right) - 2M_{xy} \frac{\partial^2 \delta w}{\partial x \partial y} + N_y \left( \frac{\partial \delta v}{\partial y} + \frac{\partial w}{\partial y} \frac{\partial \delta w}{\partial y} \right) - M_y \frac{\partial^2 \delta w}{\partial y^2} \right] dx dy - \iint_R q \delta w dx dy + \oint_r \overline{N}_v \delta u_v ds + \oint_r \overline{N}_{vs} \delta u_s ds \quad (3.2.16)$$



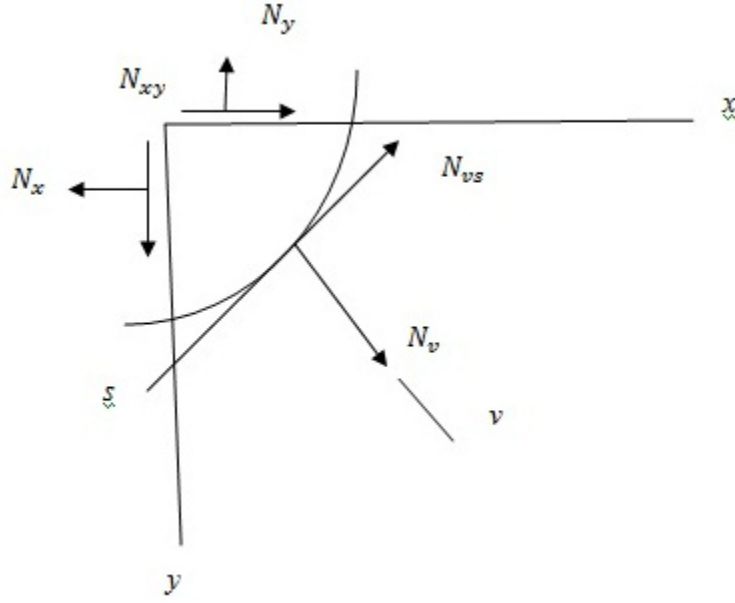


Fig. 3.2.3

We may proceed to carry out the extermination process. We employ Green's theorem one or more times to get the  $\delta u$ 's and  $\delta v$ 's out form of partial derivatives. Then we proceed to simplify the expressions in the line integrals by noting form equilibrium shown in the above figure 3.2.3.

$$N_v = N_x a_{vx}^2 + 2N_{xy} a_{vx} a_{vy} + N_y a_{vy}^2 \quad (3.2.17)$$

$$N_{vs} = (N_y - N_x) + 2N_{xy} a_{vx} a_{vy} + N_{xy} (a_{vx}^2 - a_{vy}^2) \quad (3.2.18)$$

Where  $a_{vx}$  and  $a_{vy}$  are the direction cosine of the outward normal of the boundary. Furthermore, simple vector projections permit us to say

$$\mathbf{u}_v = a_{vx} \mathbf{u} + a_{vy} \mathbf{v} \quad (3.2.19)$$

$$\mathbf{u}_s = -a_{vy} \mathbf{u} + a_{vx} \mathbf{v} \quad (3.2.20)$$

Here we also note

$$\frac{\partial}{\partial x} = a_{vx} \frac{\partial}{\partial v} - a_{vy} \frac{\partial}{\partial s} \quad (3.2.21)$$

$$\frac{\partial}{\partial y} = a_{vy} \frac{\partial}{\partial v} + a_{vx} \frac{\partial}{\partial s} \quad (3.2.22)$$

Finally we introduce the transverse shear forces of plate theory

$$Q_v = Q_x a_{vx} + Q_y a_{vy}$$

$$Q_x = \frac{\partial M_x}{\partial x} + \frac{\partial M_{xy}}{\partial y} \quad (3.2.23)$$

$$Q_y = \frac{\partial M_y}{\partial y} + \frac{\partial M_{xy}}{\partial x}$$

Now using equation 3.2.17, 3.2.18 and 3.2.23 we can write as

$$\begin{aligned} \delta^{(1)}\pi = & - \iint_R \left[ \left( \frac{\partial N_x}{\partial x} + \frac{\partial N_{xy}}{\partial y} \right) \delta u + \left( \frac{\partial N_{xy}}{\partial x} + \frac{\partial N_y}{\partial y} \right) \delta v + \left\{ \frac{\partial^2 M_x}{\partial x^2} + 2 \frac{\partial^2 M_{xy}}{\partial x \partial y} + \frac{\partial^2 M_y}{\partial y^2} + \right. \\ & \left. \frac{\partial}{\partial x} \left( N_x \frac{\partial w}{\partial x} \right) + \frac{\partial}{\partial y} \left( N_{xy} \frac{\partial w}{\partial x} \right) + \frac{\partial}{\partial x} \left( N_{xy} \frac{\partial w}{\partial y} \right) + \frac{\partial}{\partial y} \left( N_y \frac{\partial w}{\partial y} \right) + q \right] \delta w \, dx dy + \oint_r (N_v + \\ & \overline{N}_v) \delta u_v \, ds + \oint_r (N_{vs} + \overline{N}_{vs}) \delta u_s \, ds - \oint_r M_v \frac{\partial \delta w}{\partial v} \, ds + \oint_r \left( Q_v + \frac{\partial M_{vs}}{\partial s} + N_v \frac{\partial w}{\partial v} + \right. \\ & \left. N_{vs} \frac{\partial w}{\partial s} \right) \delta w \, ds - [M_{vs} \delta w]_r = 0 \end{aligned} \quad (3.2.24)$$

The last expression accounts for “corners” in the boundary. From the above equations we may now make series of deductions. First, in region R we conclude that

$$\frac{\partial N_x}{\partial x} + \frac{\partial N_{xy}}{\partial y} = 0 \quad (3.2.25a)$$

$$\frac{\partial N_{xy}}{\partial x} + \frac{\partial N_y}{\partial y} = 0 \quad (3.2.25b)$$

$$\begin{aligned} & \frac{\partial^2 M_x}{\partial x^2} + 2 \frac{\partial^2 M_{xy}}{\partial x \partial y} + \frac{\partial^2 M_y}{\partial y^2} + \frac{\partial}{\partial y} \left( N_x \frac{\partial w}{\partial x} \right) + \frac{\partial}{\partial y} \left( N_{xy} \frac{\partial w}{\partial x} \right) + \frac{\partial}{\partial x} \left( N_{xy} \frac{\partial w}{\partial y} \right) + \\ & \frac{\partial}{\partial y} \left( N_y \frac{\partial w}{\partial y} \right) + q = 0 \end{aligned} \quad (3.2.25c)$$

The first two equations above clearly are identical to the equations of equilibrium for plane stress, as is to be expected. We shall use these equations now to simplify the third equation after

we use the differentiation operators on the above expressions involving products. We are thus able to eliminate expressions involving products. We are thus able to eliminate expressions involving products. We are thus able to eliminate expressions involving the partial of  $w$ . We get

$$\frac{\partial^2 M_x}{\partial x^2} + 2 \frac{\partial^2 M_{xy}}{\partial x \partial y} + \frac{\partial^2 M_y}{\partial y^2} + N_x \frac{\partial^2 w}{\partial x^2} + 2N_{xy} \frac{\partial^2 w}{\partial x \partial y} + N_y \frac{\partial^2 w}{\partial y^2} + q = 0 \quad (3.2.26)$$

Now comparing Eq. (3.2.26) with the classical case we have here introduced nonlinear terms  $\left[ N_x \frac{\partial^2 w}{\partial x^2} + 2N_{xy} \frac{\partial^2 w}{\partial x \partial y} + N_y \frac{\partial^2 w}{\partial y^2} \right]$  involving the in-plane force intensities as additional “transverse loading”.

Considering next the remainder Eq. (3.2.24) we can stipulate the following boundary conditions along  $\Gamma$ :

$$\text{EITHER } N_v = -\overline{N}_v \text{ OR } u_v \text{ IS SPECIFIED} \quad (3.2.27a)$$

$$\text{EITHER } N_{vs} = -\overline{N}_{vs} \text{ OR } u_s \text{ IS SPECIFIED} \quad (3.2.27b)$$

$$\text{EITHER } M_v = 0 \text{ OR } \frac{\partial w}{\partial v} \text{ IS SPECIFIED} \quad (3.2.27c)$$

$$\text{EITHER } Q_v + \frac{\partial M_{vs}}{\partial s} + N_v \frac{\partial w}{\partial v} + N_{vs} \frac{\partial w}{\partial s} = 0 \text{ OR } w \text{ IS SPECIFIED} \quad (3.2.27d)$$

$$\text{At discontinuities } [M_{vs} \delta w] = 0 \quad (3.2.27e)$$

The last three conditions are familiar form work on plates except that the effective shear force  $(Q_v + \frac{\partial M_{vs}}{\partial s})$  is now augmented by projections of the in-plate forces at the plate edges.

The equations of equilibrium may be solved if a constitutive law is used. We will employ here (as pointed out earlier) the familiar Hook’s law for plane stress. We will use the constitutive law to replace the resultant intensity functions by appropriate derivatives of the displacement field of the mid plane of the plate. Consider, for example, the quantity  $M_x$ . Using Hook’s law and Eq. (3.2.10), we have

$$M_x = \int_{-h/2}^{h/2} \tau_{xx} z dz = \int_{-h/2}^{h/2} z \frac{E}{1-\mu^2} (\epsilon_{xx} + \mu \epsilon_{yy}) dz = \int_{-h/2}^{h/2} z \frac{E}{1-\mu^2} \left[ \frac{\partial u}{\partial x} - z \frac{\partial^2 w}{\partial x^2} + \frac{1}{2} \left( \frac{\partial w}{\partial x} \right)^2 + \mu \frac{\partial v}{\partial y} - z \mu \frac{\partial^2 w}{\partial y^2} + \frac{\mu}{2} \left( \frac{\partial w}{\partial y} \right)^2 \right] dz$$

Integrating and inserting limits, we get

$$M_x = \frac{E}{1-\mu^2} \frac{h^3}{12} \left( -\frac{\partial^2 w}{\partial x^2} - \mu \frac{\partial^2 w}{\partial y^2} \right) = -D \left( \frac{\partial^2 w}{\partial x^2} + \mu \frac{\partial^2 w}{\partial y^2} \right) \quad (3.2.28)$$

Where D is the familiar bending rigidity, given as  $D = \frac{Eh^3}{12(1-\mu^2)}$ , similarly we have

$$M_y = -D \left( \frac{\partial^2 w}{\partial y^2} + \mu \frac{\partial^2 w}{\partial x^2} \right) \quad (3.2.29a)$$

$$M_{xy} = -D(1-\mu) \frac{\partial^2 w}{\partial x \partial y} \quad (3.2.29b)$$

$$N_y = C \left\{ \left[ \frac{\partial u}{\partial x} + \frac{1}{2} \left( \frac{\partial w}{\partial x} \right)^2 \right] + \mu \left[ \frac{\partial v}{\partial y} + \frac{1}{2} \left( \frac{\partial w}{\partial y} \right)^2 \right] \right\} \quad (3.2.29c)$$

$$N_x = C \left\{ \left[ \frac{\partial v}{\partial y} + \frac{1}{2} \left( \frac{\partial w}{\partial y} \right)^2 \right] + \mu \left[ \frac{\partial u}{\partial x} + \frac{1}{2} \left( \frac{\partial w}{\partial x} \right)^2 \right] \right\} \quad (3.2.29d)$$

$$N_{xy} = C \left( \frac{1-\mu}{2} \right) \left[ \frac{\partial u}{\partial y} + \frac{\partial v}{\partial x} + \frac{\partial w}{\partial x} \frac{\partial w}{\partial y} \right] \quad (3.2.29e)$$

Where C is given extensional rigidity, given as

$$C = \frac{Eh}{1-\mu^2}$$

We could now substitute in Eq. (3.2.26) for the resultant intensity functions, using above relations to get the equilibrium equations in terms of displacement components of the mid plane plate. However, we shall follow another route that leads to a somewhat less complicated system of equations.

Note accordingly that Eqs. (3.2.25a) and (3.2.25b) will be individually satisfied if we define an Airy stress function F as follows:

$$N_x = \frac{\partial^2 F}{\partial y^2}$$

$$N_y = \frac{\partial^2 F}{\partial x^2} \quad (3.2.30)$$

$$N_{xy} = -\frac{\partial^2 F}{\partial x \partial y}$$

Then replacing  $M_x$ ,  $M_y$  and  $M_{xy}$ , it is a simple matter to show that Eq. (3.2.25c) can be written as

$$D\nabla^4 w = \frac{\partial^2 F}{\partial y^2} \frac{\partial^2 w}{\partial x^2} - 2 \frac{\partial^2 F}{\partial x \partial y} \frac{\partial^2 w}{\partial x \partial y} + \frac{\partial^2 F}{\partial x^2} \frac{\partial^2 w}{\partial y^2} + q \quad (3.2.31)$$

We now have a single partial differential equation with two dependent variables,  $w$  and  $F$ . since we are now studying in-plane effects by a stress approach, we must ensure the compatibility of the in-plane displacements. This will give us a second companion equation to go with Eq. (3.2.31). To do this, we shall seek to relate the strain  $\epsilon_{xx}$ ,  $\epsilon_{yy}$ , and  $\epsilon_{xy}$  at the mid plane surface in such a way that when employ Eq. (3.2.10) to replace the strains we end up with a result that does not contain the in-plane displacement components  $u$  and  $v$ . thus we you may readily demonstrate by substituting from Eq. (3.2.10) that

$$\left( \frac{\partial^2 \epsilon_{xx}}{\partial y^2} - 2 \frac{\partial^2 \epsilon_{xy}}{\partial x \partial y} + \frac{\partial^2 \epsilon_{yy}}{\partial x^2} \right)_{z=0} = \left( \frac{\partial^2 w}{\partial x \partial y} \right)^2 - \frac{\partial^2 w}{\partial x^2} \frac{\partial^2 w}{\partial y^2} \quad (3.2.32)$$

Since this equation ensures the proper relation of strains at the mid plane surface to the mid plane displacement component  $w$  without explicitly involving in-plane displacement components  $u$  and  $v$ , it serves as the desired compatibility equation for the strains at the mid plane surface. We next express the compatibility equation in terms of the stress resultant intensity function. To do this, substitute for strains, using Eq.(3.2.10) and then note Eqs.(3.2.29) stemming from Hook's law:

$$\frac{1}{Eh} \left[ \frac{\partial^2 N_x}{\partial y^2} - \mu \frac{\partial^2 N_y}{\partial y^2} + \frac{\partial^2 N_y}{\partial x^2} - \mu \frac{\partial^2 N_x}{\partial x^2} + 2(1 + \mu) \frac{\partial^2 N_{xy}}{\partial x \partial y} \right] = \left( \frac{\partial^2 w}{\partial x \partial y} \right)^2 - \frac{\partial^2 w}{\partial x^2} \frac{\partial^2 w}{\partial y^2}$$

Finally, replacing the resultant intensity functions in terms of the Airy function [see Eq. (3.2.30)], we get

$$\nabla^4 F = Eh \left[ \left( \frac{\partial^2 w}{\partial x \partial y} \right)^2 - \frac{\partial^2 w}{\partial x^2} \frac{\partial^2 w}{\partial y^2} \right] \quad (3.2.33)$$

the above equation and Eq. (3.2.31), which we now rewrite as

$$D \nabla^4 w = \frac{\partial^2 F}{\partial y^2} \frac{\partial^2 w}{\partial x^2} - 2 \frac{\partial^2 F}{\partial x \partial y} \frac{\partial^2 w}{\partial x \partial y} + \frac{\partial^2 F}{\partial x^2} \frac{\partial^2 w}{\partial y^2} + q \quad (3.2.34)$$

Are the celebrated von karman plate equations. Note that they are still highly non-linear. The equations do have considerable mutual symmetry. This is brought out by defining a nonlinear operator L:

$$L(p, q) = \frac{\partial^2 p}{\partial y^2} \frac{\partial^2 q}{\partial x^2} - 2 \frac{\partial^2 p}{\partial x \partial y} \frac{\partial^2 q}{\partial x \partial y} + \frac{\partial^2 p}{\partial x^2} \frac{\partial^2 q}{\partial y^2} \quad (3.2.35)$$

Then the von karman plate equations can be given as

$$\nabla^4 F = - \frac{Eh}{2} L(w, w) \quad (3.2.36a)$$

$$D \nabla^4 w = L(F, w) + q \quad (3.2.36b)$$

The deflection of the non linear operator leaves us with the (uncoupled) plane –stress problem of two – dimensional elasticity theory and the classic plate bending equation.

### 3.3 Strain-displacement relations

In the present formulation the strain-displacement relations are derived based on a higher-order shear deformation theory that includes the initial geometric imperfections and von Karman-type geometric nonlinearities.

The nonlinear strain-displacement relations at a distance ‘z’ away from the mid-plane of a isotropic plate can be written as:

$$\begin{aligned} \epsilon_x &= \epsilon_x^0 - z w_{,xx}^0 \\ \epsilon_y &= \epsilon_y^0 - z w_{,yy}^0 \\ \gamma_{xy} &= \epsilon_{xy}^0 - 2z \epsilon_{,xy}^0 \end{aligned} \quad (3.3.1)$$

$$\gamma_{xz} = u_{,z} + w_{,x}$$

$$\gamma_{yz} = v_{,z} + w_{,y}$$

$\epsilon_x^o$ ,  $\epsilon_y^o$  and  $\gamma_{xy}^o$  are reference surface strains and are defined as:

$$\epsilon_x^o = u_{,x}^o + \frac{1}{2}(w_{,x}^o)^2$$

$$\epsilon_y^o = u_{,y}^o + \frac{1}{2}(w_{,y}^o)^2 \quad (3.3.2)$$

$$\gamma_{xy}^o = u_{,y}^o + v_{,x}^o + w_{,x}^o w_{,y}^o$$

For a slightly imperfect plate let  $w^*$  denote a known small geometric imperfection, i.e., a small deviation of the plate middle-surface from the mid-plane of a perfect plate. The unloaded imperfect plate is assumed to be stress free. In the case of imperfect plate,  $w^o$  is measured from the load free imperfect middle-surface. The geometric imperfection of a plate based on fundamental buckling mode of a geometrically perfect plate is assumed as:

$$w^* = e \sin \frac{\pi x}{a} \sin \frac{\pi y}{b}$$

The coefficient  $e$  represents amplitude of the initial imperfection. The initial strains due to the imperfection can be written as

$$\epsilon_x^* = \frac{1}{2}(w_{,x}^*)^2; \quad \epsilon_y^* = \frac{1}{2}(w_{,y}^*)^2;$$

$$\gamma_{xy}^* = w_{,x}^* w_{,y}^* ; \quad (3.3.3)$$

$$\gamma_{xz}^* = w_{,x}^*; \quad \gamma_{yz}^* = w_{,y}^*;$$

The net strain component in the middle surface of the imperfect plate become (small angles of rotation  $w_{,x}^*$  in the equations for an initially perfect plate are replaced by  $(w^* + w^o)_{,x}$  :

$$\bar{\epsilon}_x^o = u_{,x}^o + \frac{1}{2} [(w^* + w^o)_{,x}^2] - \epsilon_x^* = (\epsilon_x^o + w_{,x}^o w_{,x}^*)$$

$$\bar{\epsilon}_y^o = v_{,y}^o + \frac{1}{2} [(w^* + w^o)_{,y}^2] - \epsilon_y^* = (\epsilon_y^o + w_{,y}^o w_{,y}^*) \quad (3.3.4)$$

$$\bar{\gamma}_{xy}^o = u_{,y}^o + v_{,x}^o + [(w^* + w^o)_{,x} (w^* + w^o)_{,y}] - \gamma_{xy}^* = (\gamma_{xy}^o + w_{,x}^o w_{,y}^* + w_{,x}^* w_{,y}^o)$$

Introducing Eqs. (3.3.4) into Eqs. (3.3.1) (i.e., replacing  $\epsilon_x^o$ ,  $\epsilon_y^o$  and  $\gamma_{xy}^o$  with  $\bar{\epsilon}_x^o$ ,  $\bar{\epsilon}_y^o$  and  $\bar{\gamma}_{xy}^o$ ), the strain components of the imperfect plate is written as:

$$\bar{\epsilon}_x = \epsilon_x^o + w_{,x}^o w_{,x}^* - zw_{,xx}^*$$

$$\bar{\epsilon}_y = \epsilon_y^o + w_{,y}^o w_{,y}^* - zw_{,yy}^*$$

$$\bar{\gamma}_{xy} = \gamma_{xy}^o + w_{,x}^o w_{,y}^* + w_{,x}^* w_{,y}^o - 2zw_{,xy}^o \quad (3.3.5)$$

$$\bar{\gamma}_{xz} = u_{,z} + w_{,x}$$

$$\bar{\gamma}_{yz} = v_{,z} + w_{,y}$$

### 3.4 Method of Solution

#### 3.4.1 Galerkin's method

Approximate solutions for the partial differential equations can be obtained using the Galerkin method, which is briefly outlined below:

An approximate solution ( $\tilde{u}^o$ ,  $\tilde{v}^o$ ,  $\tilde{w}^o$ ) of the problem is sought in the form

$$\tilde{u}^o = \sum_{m=1}^i \sum_{n=1}^j U_{mn} \bar{a}_{mn} (x, y)$$

$$\tilde{v}^o = \sum_{m=1}^i \sum_{n=1}^j V_{mn} \bar{b}_{mn} (x, y)$$

$$\tilde{w}^o = \sum_{m=1}^i \sum_{n=1}^j W_{mn} \bar{c}_{mn} (x, y)$$

(3.4.1.1)



Where  $U_{mn}$ ,  $V_{mn}$  and  $W_{mn}$  are undetermined coefficients and  $\bar{a}_{mn}$ ,  $\bar{b}_{mn}$  and  $\bar{c}_{mn}$  are suitably chosen spatial functions satisfying the prescribed boundary conditions. Then the Galerkin method implies

$$\begin{aligned}\iint L_1(\tilde{u}^o, \tilde{v}^o, \tilde{w}^o) \bar{a}_{mn}(x,y) dx dy &= 0 \\ \iint L_1(\tilde{u}^o, \tilde{v}^o, \tilde{w}^o) \bar{b}_{mn}(x,y) dx dy &= 0 \\ \iint L_1(\tilde{u}^o, \tilde{v}^o, \tilde{w}^o) \bar{c}_{mn}(x,y) dx dy &= 0\end{aligned}\quad (3.4.1.2)$$

Where the integration is carried out over the entire shell area. There will be as many equations (in  $L_i$ ) as the number of terms taken for the series given by Eqs. (3.4.1.2).

### 3.4.2 Boundary conditions and displacement fields

It is presumed that all four edges of the plate or shell are simply supported. The following three sets of simply supported boundary conditions are considered in the present study.

**3.4.2.1 only normal in-plane displacements can occur (SS-1):** In-plane tangential displacements and out-of-plane displacements are prevented.

$$\begin{aligned}N_x = v^o = w^o = M_x = 0 \text{ at } x = 0, a \\ N_y = u^o = w^o = M_x = 0 \text{ at } x = 0, b\end{aligned}\quad (3.4.2.1a)$$

The following displacement fields are used to satisfy the above set of boundary conditions:

$$\begin{aligned}\tilde{u}^o &= \sum_{m=1}^M \sum_{n=1}^N U_{mn} \cos \frac{m\pi x}{a} \sin \frac{n\pi y}{b} \\ \tilde{v}^o &= \sum_{m=1}^M \sum_{n=1}^N V_{mn} \sin \frac{m\pi x}{a} \cos \frac{n\pi y}{b}\end{aligned}$$

$$\tilde{w}^o = \sum_{m=1}^M \sum_{n=1}^N W_{mn} \sin \frac{m\pi x}{a} \sin \frac{n\pi y}{b}$$

(3.4.2.1b)

**3.4.2.2 Immovable edges (SS-2):** In-plane normal and tangential displacements and out-of-plane displacements are prevented.

$$u^o = v^o = w^o = M_x = 0 \text{ at } x=0, a$$

$$v^o = u^o = w^o = M_x = 0 \text{ at } x=0, b$$

(3.4.2.2a)

The following displacement fields are used to satisfy the above set of boundary conditions:

$$\tilde{u}^o = \sum_{m=1}^M \sum_{n=1}^N U_{mn} \sin \frac{2m\pi x}{a} \sin \frac{n\pi y}{b}$$

$$\tilde{v}^o = \sum_{m=1}^M \sum_{n=1}^N V_{mn} \sin \frac{m\pi x}{a} \sin \frac{2n\pi y}{b}$$

$$\tilde{w}^o = \sum_{m=1}^M \sum_{n=1}^N W_{mn} \sin \frac{m\pi x}{a} \sin \frac{n\pi y}{b}$$

(3.4.2.2b)

**3.4.2.3 only tangential displacements can occur (SS-3):** In-plane normal displacements and out-of-plane displacements are prevented.

$$N_{xy} = v^o = w^o = M_x = 0 \text{ at } x=0, a$$

$$N_{xy} = u^o = w^o = M_x = 0 \text{ at } x=0, b$$

(3.4.2.3a)

The following displacement fields are used to satisfy the above set of boundary conditions:

$$\tilde{u}^o = \sum_{i=1}^m \sum_{j=1}^n U_{ij} \sin \frac{i\pi x}{a} \cos \frac{j\pi y}{b}$$

$$\tilde{v}^o = \sum_{i=1}^m \sum_{j=1}^n V_{ij} \cos \frac{i\pi x}{a} \sin \frac{j\pi y}{b}$$

$$\tilde{w}^o = \sum_{i=1}^m \sum_{j=1}^n W_{ij} \sin \frac{i\pi x}{a} \sin \frac{j\pi y}{b}$$

(3.4.2.3a)

### 3.5 Solution of a non-linear equation

Equations that can be cast in the form of a polynomial are referred to as algebraic equations. Equations involving more complicated terms, such as trigonometric, hyperbolic, exponential, or logarithmic functions are referred to as transcendental equations. The methods presented in this section are numerical methods that can be applied to the solution of such equations, to which we will refer, in general, as non-linear equations. In general, we will be searching for one, or more, solutions to the equation,

$$f(x) = 0.$$

We will present the *Newton-Raphson* method. In the Newton-Raphson methods only one initial value is required. Because the solution is not exact, the algorithms for any of the methods presented herein will not provide the exact solution to the equation  $f(x) = 0$ , instead, we will stop the algorithm when the equation is satisfied within an allowed tolerance or error,  $\epsilon$ . In mathematical terms this is expressed as

$$|f(xR)| < \epsilon.$$

The value of  $x$  for which the non-linear equation  $f(x)=0$  is satisfied, i.e.,  $x = xR$ , will be the solution, or root, to the equation within an error of  $\epsilon$  units.

### 3.5.1 The Newton-Raphson method

Consider the Taylor-series expansion of the function  $f(x)$  about a value  $x = x_0$ :

$$f(x) = f(x_0) + f'(x_0)(x-x_0) + \frac{f''(x_0)}{2!}(x-x_0)^2 + \dots$$

Using only the first two terms of the expansion, a first approximation to the root of the equation

$$f(x) = 0$$

can be obtained from

$$f(x) = 0 \approx f(x_0) + f'(x_0)(x_1 - x_0)$$

Such approximation is given by,

$$x_1 = x_0 - f(x_0)/f'(x_0).$$

The Newton-Raphson method consists in obtaining improved values of the approximate root through the recurrent application of equation above. For example, the second and third approximations to the equation here that root will be given by

$$x_2 = x_1 - f(x_1)/f'(x_1),$$

and

$$x_3 = x_2 - f(x_2)/f'(x_2),$$

respectively.

This iterative procedure can be generalized by writing the following equation, where  $i$  represents the iteration number:

$$x_{i+1} = x_i - f(x_i)/f'(x_i).$$

After each iteration the program should check to see if the convergence condition, namely,

$$|f(x_{i+1})| < \epsilon,$$

is satisfied.

The figure below illustrates the way in which the solution is found by using the Newton-Raphson method. Notice that the equation  $f(x) = 0 \approx f(x_0) + f'(x_0)(x_1 - x_0)$  represents a straight line tangent to the curve  $y = f(x)$  at  $x = x_0$ . This line intersects the  $x$ -axis (i.e.,  $y = f(x) = 0$ ) at the point  $x_1$  as given by  $x_1 = x_0 - f(x_0)/f'(x_0)$ . At that point we can construct another straight line tangent to  $y = f(x)$  whose intersection with the  $x$ -axis is the new approximation to the root of  $f(x) = 0$ , namely,  $x = x_2$ . Proceeding with the iteration we can see that the intersection of consecutive tangent lines with the  $x$ -axis approaches the actual root relatively fast.

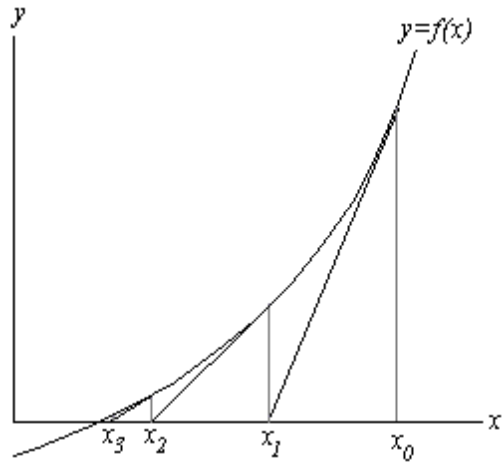


Fig no -3.5.1

The Newton-Raphson method converges relatively fast for most functions regardless of the initial value chosen. The main disadvantage is that you need to know not only the function  $f(x)$ , but also its derivative,  $f'(x)$ , in order to achieve a solution.

## 4 Numerical Results and Discussion: Plates

### 4.1 Introduction

The mathematical formulation presented in previous chapter is applicable for buckling and postbuckling of isotropic plates. In this chapter, the numerical results validating the analytical formulation for buckling and postbuckling of isotropic plates by using MAT Lab are presented in this chapter. In this chapter the uniaxial loads are presented here in details.

### 4.2 Boundary conditions

All numerical results presented in this chapter are for simply supported isotropic plates, composed of equal thickness of homogenous material. Depending upon the in-plane displacement constraint at edges, following three sets of simply supported boundary conditions are considered in the present study.

**4.2.1 Only normal in-plane displacements can occur (SS-1):** In-plane tangential displacements and out-of-plane displacements are prevented.

$$N_x = v^o = w^o = M_x = 0 \text{ at } x = 0, a$$

$$N_y = u^o = w^o = M_y = 0 \text{ at } x = 0, b$$

**4.2.2 Immovable edges (SS-2):** In-plane normal and tangential displacements and out-of-plane displacements are prevented.

$$u^o = v^o = w^o = M_x = 0 \text{ at } x = 0, a$$

$$v^o = u^o = w^o = M_y = 0 \text{ at } x = 0, b$$

**4.2.3 Only tangential displacements can occur (SS-3):** In-plane normal displacements and out-of-plane displacements are prevented.

$$N_{xy} = v^o = w^o = M_x = 0 \text{ at } x = 0, a$$

$$N_{xy} = u^o = w^o = M_y = 0 \text{ at } x = 0, b$$

Where  $a$  and  $b$  are the plate lengths in the  $x$ - and  $y$ -directions, respectively. The displacement fields appropriate to the above set of boundary conditions (SS-1, SS-2, SS-3) are specified in Mathematical formulation.

#### 4.2.4 Number of terms in the displacement fields:

In order to examine the convergence of the present multi-term Galerkin's solution, an extensive numerical study using different numbers of terms in the assumed displacement fields was performed. The following different numbers of terms were used along  $x$  and  $y$  directions in the displacement field approximation.

one-term:  $(m = 1, n = 1)$

two-term:  $(m = 1, n = 1), (m = 3, n = 1)$

three-term:  $(m = 1, n = 1), (m = 3, n = 1), (m = 1, n = 3)$

four-term:  $(m = 1, n = 1), (m = 3, n = 1), (m = 1, n = 3), (m = 3, n = 3)$

six-term:  $(m = 1, n = 1), (m = 3, n = 1), (m = 1, n = 3), (m = 3, n = 3),$   
 $(m = 5, n = 1), (m = 1, n = 5)$

nine-term:  $(m = 1, n = 1), (m = 1, n = 3), (m = 1, n = 5), (m = 3, n = 1),$   
 $(m = 3, n = 3), (m = 3, n = 5), (m = 5, n = 1), (m = 5, n = 3),$   
 $(m = 5, n = 5)$

sixteen-term:  $(m = 1, n = 1), (m = 1, n = 3), (m = 1, n = 5), (m = 1, n = 7),$   
 $(m = 3, n = 1), (m = 3, n = 3), (m = 3, n = 5), (m = 3, n = 7),$   
 $(m = 5, n = 1), (m = 5, n = 3), (m = 5, n = 5), (m = 5, n = 7),$   
 $(m = 7, n = 1), (m = 7, n = 3), (m = 7, n = 5), (m = 7, n = 7)$

### 4.3 Buckling of Isotropic plates subjected to a Uniaxial compressive force :

Our aim is to find critical buckling load of simply supported plate by using Galerkin method. We also use the MAT LAB programming to finding eigen value for algebraic equation which gives the critical buckling load. We plot the graph between aspect ratio (a/b) and Numerical factor (k) by using the MAT LAB programming and find different modes and different aspect ratio. The critical buckling load is given by

$$\bar{N}_{xcr} = 4 \frac{\pi^2 D}{b^2}$$

For other proportions of the plate the  $\bar{N}_x$  can be represented in the form

$$\bar{N}_x = \frac{k\pi^2 D}{b^2}$$

Where k is a numerical factor,

The following properties of plate are used  $h=1/100, \mu =0.25, E= 200$  Gpa. The graph plotted between variation of Numerical factor (k) and aspect ratio (a/b) is shown in the fig. 4.3.1. from the given figure we found that if we increase the aspect ratio different modes are found . In the point where aspect ratio  $a/b = 1.4$  the mode is changing from  $m = 1$  to  $m =2$ . It is also observed from figure for very long aspect ratio ( $a/b > 5$ ) plate buckling modes are remain same. The result is compared with Theory of elastic stability by Timoshenko & Gere of page no 353, fig no 9.2.



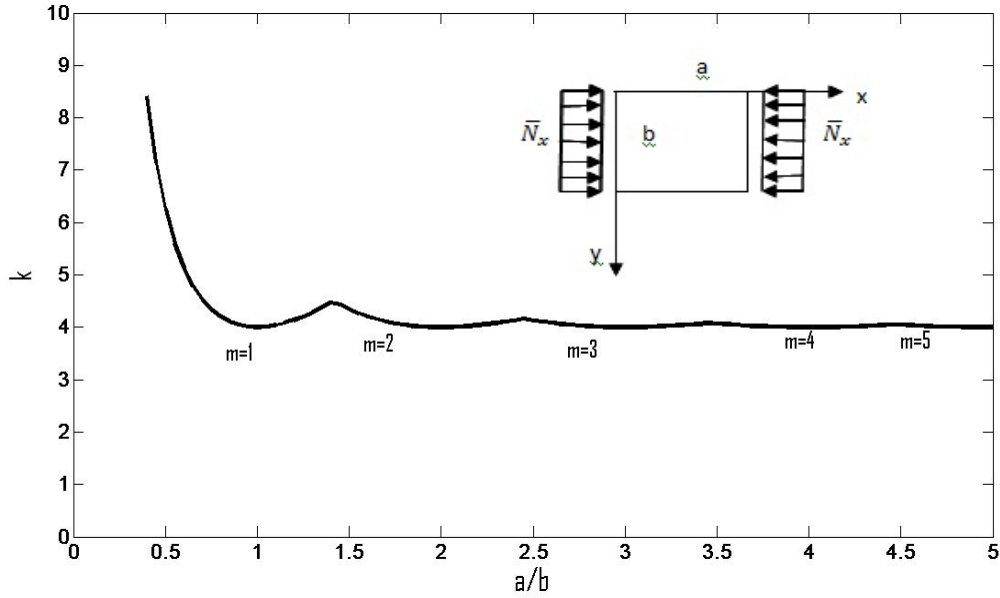


Fig 4.3.1 Variation of buckling coefficient of a SS-1 plate under Uniaxial inplane loading for different aspect ratio ( $a/b$ ) and  $k$  value

#### 4.4 Postbuckling behavior of Isotropic plates

##### 4.4.1 Isotropic plates subjected to a Uniaxial Compressive force

The postbuckling behavior isotropic plates subjected to in-plane compressive loads are studied here. Numerical results are presented for Isotropic plates. The simply supported (SS-1) boundary conditions are considered on all four edges of the plate. The material properties used for isotropic plate are:  $E = 200\text{Gpa}$ ,  $\mu=0.25$

The postbuckled equilibrium paths of a isotropic square plate (length-to-thickness ratio  $a/h = 100$ ), subjected to in-plane uniform edge compression are shown in Fig. 4.4.1, and 4.4.2. The plate center deflections ( $w$ ) are normalized with the thickness of the plate ( $h$ ) and the compressive force ( $\bar{N}_x$ ) is normalized with the critical buckling load of the plate ( $\bar{N}_{xcr}$ ). The equilibrium paths are obtained by taking 1-term, 3-terms, 4-terms and 9-terms in the displacement field approximation. For the compressive load up to  $\bar{N}_x / \bar{N}_{xcr} = 2$ , the postbuckled deflections obtained from the 1-term solution and multi-term (3-term, 4-term and 9-term) solution are in good agreement. The results indicate that at higher magnitude of uniaxial compressive loads the one-term solution is erroneous and the discrepancy between the 1-term

and multi-term solution is noticeable. At a load  $\bar{N}_x / \bar{N}_{xcr} = 5$ , the difference in the central deflections as calculated by considering 1-term and multi-term solution is 9.6%, whereas at  $\bar{N}_x / \bar{N}_{xcr} = 10$ , the difference is 17.5%. It is observed that even at  $\bar{N}_x / \bar{N}_{xcr} = 10$ , the discrepancy between the 3-terms and multi-term (4-term and 9-term) solution is less than 2%. Thus, a minimum of 3-terms is required to obtain accurate results for the problem under consideration. Unless stated otherwise, all further numerical results of plates are obtained using 3-terms in the displacement field approximation.

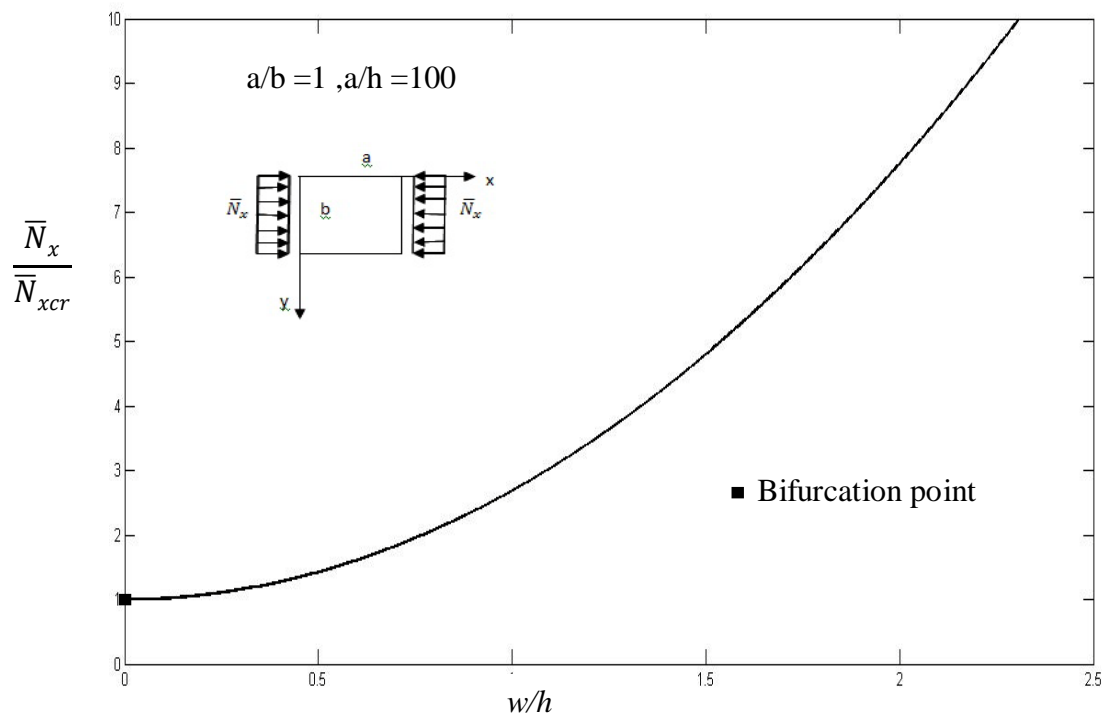


**Fig. 4.4.1** Postbuckled path of plate at central deflection versus uniaxial compressive load of a Isotropic by taking 1 term square plate.

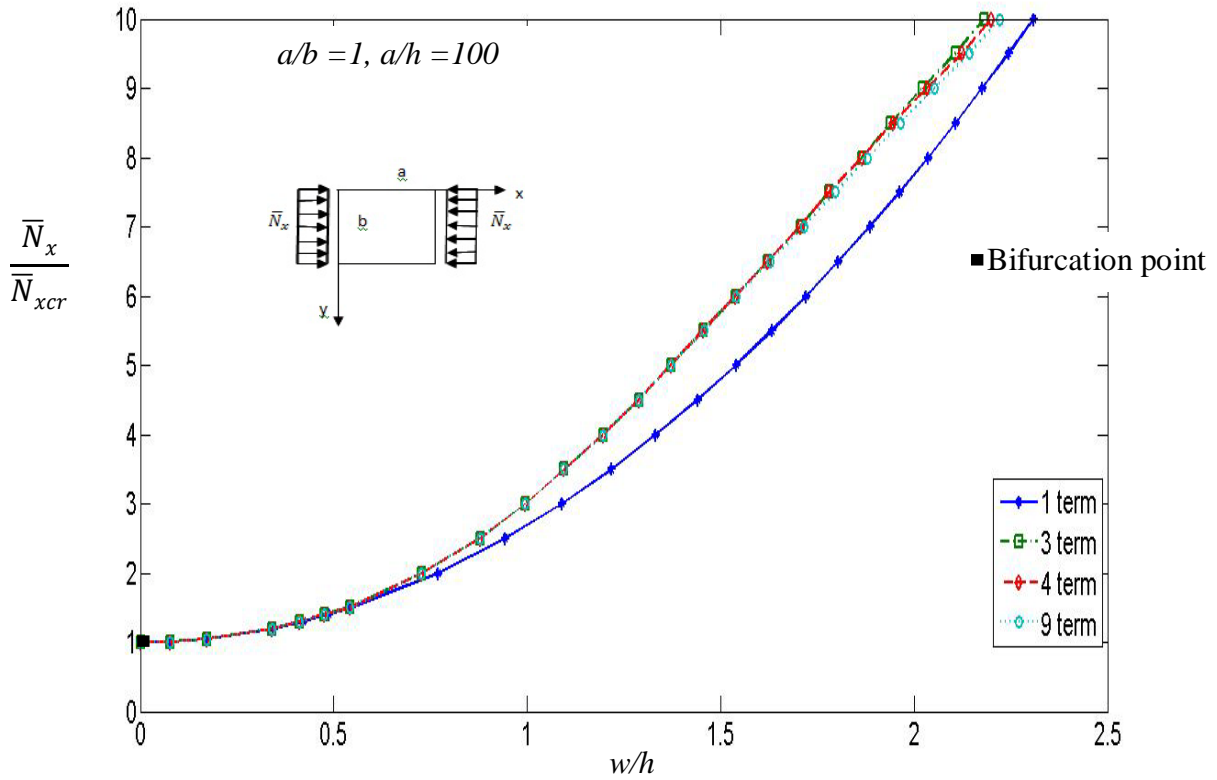


**Fig. 4.4.2** Variation of the postbuckled path of plate at central deflection versus uniaxial compressive load of a isotropic square plate.

Fig. 4.4.3 shows the postbuckled equilibrium paths of a rectangular ( $b/a = 2, a/h = 100$ ) isotropic plate subjected to a uniaxial compressive force. The equilibrium paths are obtained by taking 1-term, 3-term, 4-term, 9-term and 16-term in the displacement field approximation. It is observed from the figure that, the 3-term and 4-term solutions under estimate the plate deflections as compared to 9-term and 16-term solutions. It is observed that up to a compressive load  $\bar{N}_x / \bar{N}_{xcr} = 10$ , minimum 6-terms are necessary to obtain accurate results.

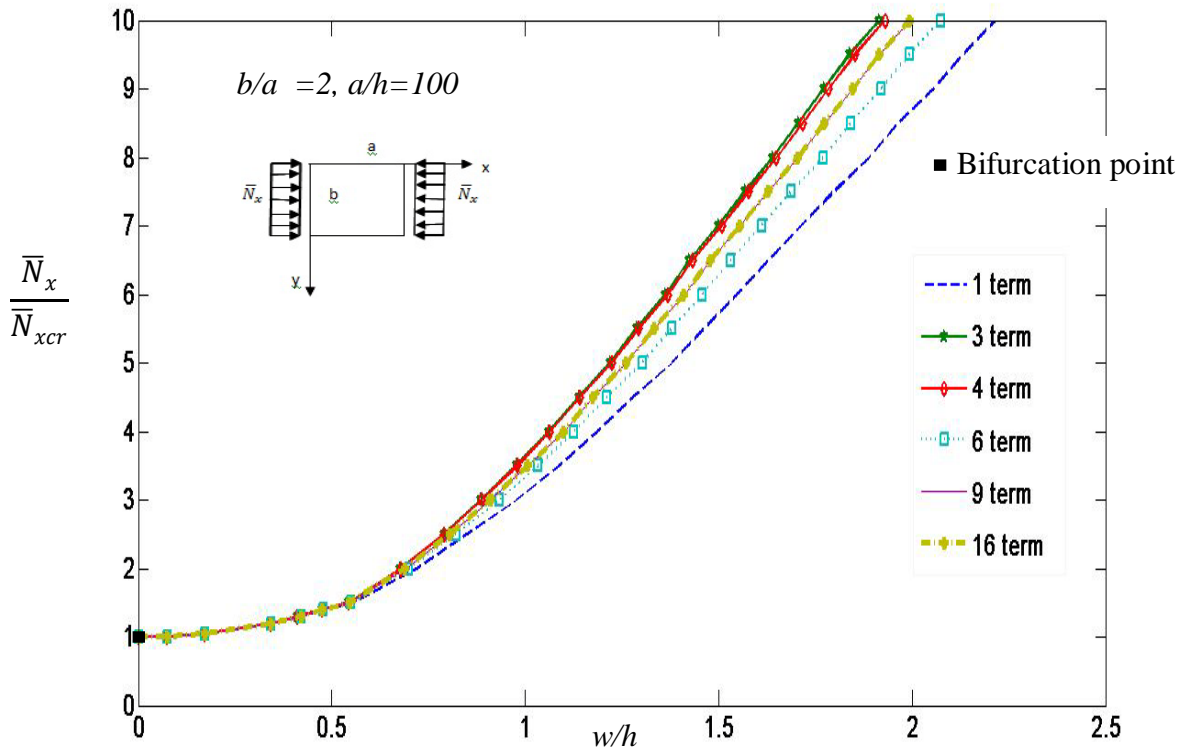


**Fig. 4.4.3** Variation of the postbuckled path of plate at central deflection versus uniaxial compressive force of a Isotropic rectangular plate.

#### 4.4.2 Response of plates subjected to uniaxial compressive load in the presence of geometric imperfections:

The response of isotropic plates subjected to uniaxial compressive loads in the presence of initial geometric imperfections is shown in Figs. 4.4.4. The plates have aspect ratio  $a/b = 1$  and length-to-thickness ratio  $a/h = 100$ . Two sets of equilibrium paths are shown in figures for positive (+ $e$ ) and negative (- $e$ ) initial imperfection magnitudes  $e = 0.025h, 0.05h, 0.1h, \text{ and } 0.2h$ . The dotted curves shown in figures are for the geometrically perfect plate ( $e = 0$ ) subjected to uniaxial compressive loads and are representative of a classic stable, symmetric bifurcation behavior. It is observed from the figures that, the introduction of an initial geometric imperfection destroy the trivial equilibrium path, and we have now a family of stable equilibrium curves corresponding to

different values of imperfection magnitudes ( $e$ ) that round off the bifurcation of the perfect system.

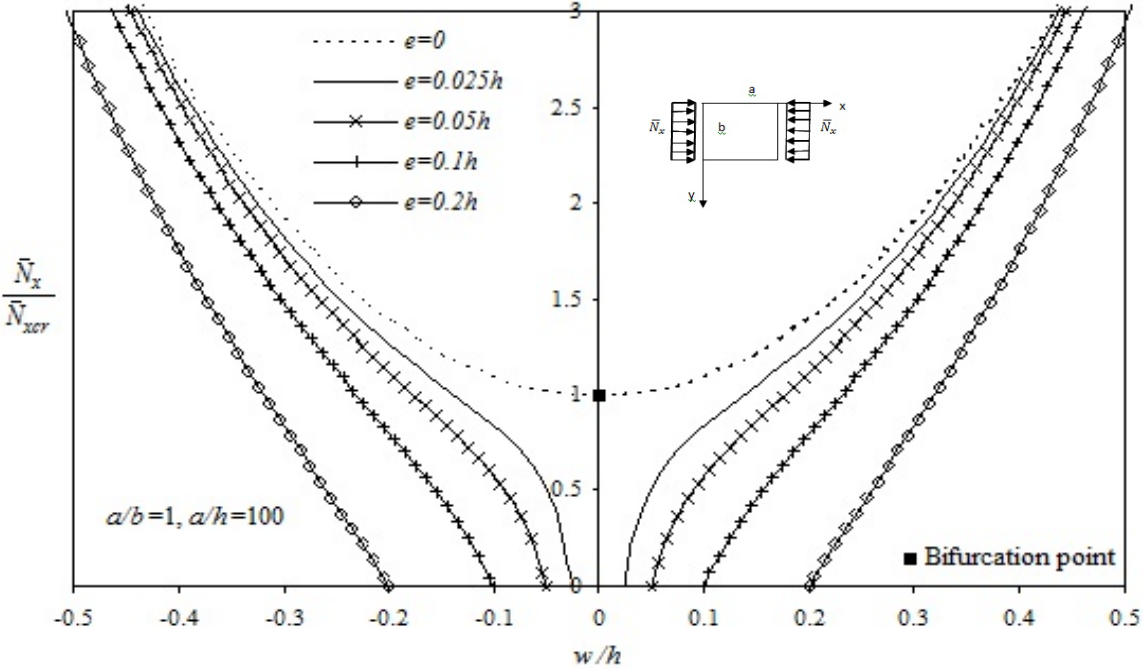


**Fig. 4.4.4** The influence of initial geometric imperfections on the nonlinear response of a square isotropic plate subjected to uniaxial compressive force

## **5. Conclusion:**

In this study the multi-term Galerkin's method is employed to investigate the buckling and postbuckling of isotropic plates subjected to uniaxial loads considering Von Karmon theory of plates. Based on the numerical work reported the following major conclusions are drawn.

1. It is observed that plate buckle in different mode up to aspect ratio five, If we increase the aspect ratio more than five the buckling mode remains same.
2. It is observed that higher postbuckling load the one-term representation of the displacement field is incorrect .The displacement result is much difference when the aspect ratio of the isotropic plate is more. In the present observation the results is studied by including up to sixteen terms in the displacement field approximation for the case of isotropic plates. For the most of the problems considered in this study the three-term representation of the displacement field are found to be sufficient. However, it is necessary to investigate the more number of terms in the displacement field.
3. In the case of plates, the initial geometric imperfections both inward (positive) and outward (negative) destroy the trivial symmetrical equilibrium path, and a family of stable equilibrium curves corresponding to different amplitudes of imperfection that round off the bifurcation of the perfect system are obtained.

## 6.Reference:

**Bhavikatti S.S.**, 2005. *Finite Element Analysis*, New Age International Publisher,

**Chia, C.Y.**, 1980. *Nonlinear Analysis of Plates*, McGraw Hill, New York.

**Chia, C.Y.**, 1988. Geometrically nonlinear behaviour of composite plates, *A review, Applied Mechanics Reviews*, 41, 439–450.

**Girish, J. Ramachandra, L.S.**, 2005. Thermal postbuckled vibrations of symmetrically laminated composite plates with initial geometric imperfections. *Journal of sound and vibration*, 282(3-5), 1137–53.

**Girish, J. Ramachandra, L.S.**, 2006. Thermo Mechanical postbuckling analysis of cross-ply laminated cylindrical shell panels. *J Engg Mech*, 132(2), 133-40.

**Grewal.**,1992 *Higher Engineering Mathematics* , Khana Publisher,

**Reddy, J.N.**, 2004. *Mechanics of Laminated Composite Plates and Shells*, Theory and Analysis, CRC Press, Boca Raton, FL, Second Edition.

**Shames and Dym.**,1991 *Finite element Method in Structural Mechanics*, New age International Publisher.

**Sarat Kumar Panda and L.S.Ramachandra.**, 2010. Buckling of rectangular plates with various boundary conditions loaded by non-uniform inplane loads, *International Journal of Mechanical Sciences*, 52, 819-828.

**L.S. Ramachandra and Sarat Kumar Panda.**, 2011. Dynamic instability of composite plates subjected to non-uniform in-planeloads, *Journal of Sound and Vibration*, 331, 53-65.

**Sarat Kumar Panda and L. S. Ramachandra.**, 2011. Buckling and Postbuckling Behavior of Cross-Ply Composite Plate Subjected to Non-uniform In-Plane Loads, *American Society for Civil Engineers*, 137(9), 589-597.

**Timoshenko, S.P. and Gere, J.M.**, 1961. *Theory of elastic stability*, McGraw-Hill, New delhi

**Timoshenko and Krieger.**, 1959. *Theory of plates and shells* , McGraw-Hill, New delhi